Effects of familial hemiplegic migraine type 1 mutations on neuronal P/Q-type Ca^{2+} channel activity and inhibitory synaptic transmission

Yu-Qing Cao and Richard W. Tsien*

Department of Molecular and Cellular Physiology, Beckman Center, Stanford University School of Medicine, Stanford, CA 94305-5345

Contributed by Richard W. Tsien, December 30, 2004

Inhibitory synapses play key roles in the modulatory circuitry that regulates pain signaling and generation of migraine headache. A rare, dominant form of this common disease, familial hemiplegic migraine type 1 (FHM1), arises from missense mutations in the pore-forming α_{1A} subunit of P/Q-type Ca^{2+} channels. These channels are normally vital for presynaptic Ca^{2+} entry and neurotransmitter release at many central synapses, raising questions about effects of FHM1 mutations on neuronal Ca^{2+} influx and inhibitory and excitatory neurotransmission. We have expressed the four original FHM1 mutant channels in hippocampal neurons from α_{1A} knockout mice. Whole-cell recordings indicated that FHM1 mutant channels were less effective than wild-type channels in their ability to conduct P/Q-type current, but not generally different from wild type in voltage-dependent channel gating. Ca^{2+} influx triggered by action potential waveforms was also diminished. In keeping with decreased channel activity, FHM1 mutant channels were correspondingly impaired in supporting the P/Q-type component of inhibitory neurotransmission. When expressed in wild-type inhibitory neurons, FHM1 mutant channels reduced the contribution of P/Q-type channels to GABAergic synaptic currents, consistent with a competition of mutant and endogenous channels for P/Q-specific slots. In all cases, N-type channels took up the burden of supporting transmission and homeostatic mechanisms maintained overall synaptic strength. The shift to reliance on N-type channels greatly increased the susceptibility to G protein-coupled modulation of neurotransmission, studied with the $GABA_B$ agonist baclofen. Thus, mutant-expressing synapses might be weakened in a heightened state of neuromodulation like that provoked by triggers of migraine such as stress.

action potential waveform | inhibitory hippocampal neuron

Migraine, the most common neurological disease (1, 2), can be associated with subclinical deficiencies in synaptic transmission in certain migraineurs (3). The hypothesis that migraine may be a synaptic disease has gained further credence through pioneering studies of familial hemiplegic migraine type 1 (FHM1), a rare hereditary form of migraine, and the identification of mutations in a neuronal Ca^{2+} channel vital for neurotransmission (4). The affected CACNA1A gene encodes the pore-forming α_{1A} subunit of the P/Q-type channel ($Ca_V2.1$), a predominant mediator of voltage-gated Ca^{2+} entry and transmitter release at many synapses in the central nervous system (5–9). Alterations in synaptic signaling are of likely importance for cross-talk between an ascending pain transmission pathway and inhibition by a powerful descending modulatory system, interactions that ultimately govern the generation of headache pain (10, 11). Despite extensive study of the role of P/Q-type channels in pain circuits (12, 13) and the impact of FHM1 mutations on P/Q-type channels (14–20), several important questions have not yet been addressed. What are the effects of FHM1 mutations on inhibitory neurotransmission and how might they be related to changes in biophysical properties of the P/Q-type channel and action potential-triggered Ca^{2+} entry? Do FHM1-related changes in P/Q-type channels alter the contributions of other neuronal Ca^{2+} channels? Do such alterations influence the way that synaptic transmission might be modulated, pertinent to neurohormonal states that favor the triggering of migraine? Answering these questions would help provide a foundation for a bottom-up approach to the pathophysiology of FHM1.

Materials and Methods

Human α_{1A} Constructs. The wild-type human (WT) human α_{1A} cDNA used in this study encodes the BI-1 (V1) splice variant (21). Individual FHM1 mutations were generated by PCR mutagenesis (Stratagene) as described (18).

Cell Culture and Transfection. Wild-type ($\alpha_{1A}{}^{+/+}$) and α_{1A} knockout ($\alpha_{1A}{}^{-/-}$) pups were generated by heterozygote crosses in accordance with the guidelines of the Animal Care and Use Committee of Stanford University. Hippocampal neurons were cultured from 1-day-old pups as described (18). Individual human α_{1A} constructs were cotransfected with pEGFPC1 plasmid (1:1 molar ratio) into 5-days *in vitro* (DIV) cultures by using a calcium phosphate method (18).

Electrophysiology. Transfected neurons were identified by EGFP fluorescence under an inverted microscope. Whole-cell patch-clamp recordings were performed at room temperature with an Axopatch 200A amplifier (Axon Instruments, Union City, CA). PCLAMP 8.2 (Axon Instruments) was used to acquire and analyze data. Signals were filtered at 1 kHz and digitized at 10 kHz. Whole-cell Ba^{2+} current and synaptic current recordings were performed as described (18). Details of solution composition and drug application are provided in *Supporting Text*, which is published as supporting information on the PNAS web site.

Ba^{2+} Current Recording. Transfected neurons were recorded between 7 and 11 DIV, with 10 mM Ba^{2+} in the extracellular solution. Neurons were voltage-clamped at −80 mV and test pulses were applied every 10 s. For each neuron, the peak current was normalized by the membrane capacitance (a measure of cell surface area) to reflect current density.

Generation of Action Potential Waveform (APW) and Ca^{2+} Current Recording. Spontaneous action potentials in hippocampal neurons were recorded under whole-cell current-clamp mode and modified in shape to have a faster rising phase to mimic action potentials at presynaptic terminals (see Fig. 3*A*). This APW was used as a command signal to elicit Ca^{2+} influx through voltage-

Freely available online through the PNAS open access option.

Abbreviations: FHM1, familial hemiplegic migraine type 1; APW, action potential waveform; DIV, days *in vitro*; HVA, high voltage-activated; EPSC, excitatory postsynaptic current; IPSC, inhibitory postsynaptic current; ω-Aga-IVA, ω-agatoxin-IVA; WT, RQ, TM, VA, and IL, human wild-type α_{1A} subunits and those with individual FHM1 mutation R192Q, T666M, V714A, and I1811L.

*To whom correspondence should be addressed. E-mail: rwtsien@stanford.edu.

www.pnas.org/cgi/doi/10.1073/pnas.0409896102

gated Ca^{2+} channels (4 mM external Ca^{2+}). All other recording conditions were the same as in Ba^{2+} current recordings.

Excitatory and Inhibitory Synaptic Transmission. Recordings were made from transfected low-density cultures (~5,000 cells per coverslip) between 12 and 18 DIV. The recording chamber was perfused with Tyrode solution (0.5 ml/min) containing 4 mM $CaCl_2$ or $MgCl_2$. A nonfluorescent neuron in close proximity to the transfected, EGFP-positive neuron was chosen as its possible postsynaptic target. Both neurons were voltage-clamped at −70 mV. The transfected, presynaptic neuron was depolarized to 0 mV for 1 ms to elicit action potentials once every 10 s. Correspondingly, an excitatory postsynaptic current (EPSC) or inhibitory postsynaptic current (IPSC) could be recorded at the untransfected, postsynaptic neuron. Peak EPSC/IPSC amplitude under each pharmacological condition was measured as the average of 20 traces. Details of the drug concentration and application procedures are described in *Supporting Text*.

Statistical Analysis. All data are reported as mean ± SEM. Statistical significance was tested by using ANOVA) with a post hoc Bonferroni test. The nonparametric Kolmogorov–Smirnov test was used to compare IPSC amplitudes between two groups.

Results

Total and P/Q-Mediated Ba^{2+} Current Densities Were Significantly Reduced in Neurons Expressing FHM1 Mutant Channels. The four original FHM1 mutations described by Ophoff *et al.* (4) (R192Q, T666M, V714A, and I1811L; RQ, TM, VA, and IL, respectively in Fig. 1*A*) all resulted in decreased P/Q-type current densities when studied in $\alpha_{1A}^{-/-}$ neurons (17, 18). Because most neurons express multiple types of high voltage-activated (HVA) Ca^{2+} channels (L-, N-, P/Q-, and R-types) (22), we asked whether other Ca^{2+} channels undergo regulation to compensate for reduced P/Q current in neurons expressing FHM1 mutants, as occurs in certain $\alpha_{1A}^{-/-}$ cerebellar neurons (23, 24).

Following the same strategy as in our previous study (18), we expressed human WT or FHM1 mutant α_{1A} subunits in cultured $\alpha_{1A}^{-/-}$ hippocampal neurons and measured whole-cell Ca^{2+} channel currents at 7–11 DIV, using 10 mM Ba^{2+} as the charge carrier (Fig. 1*B*). Neurons expressing mutant channels suffered a ~50% reduction of total Ba^{2+} current density relative to those expressing WT P/Q-type channels across a broad voltage range (0 to +50 mV). This finding indicated that other Ca^{2+} channels did not fully make up for the reduction of P/Q-type current in FHM1 mutant-expressing neurons.

To evaluate the current densities supported by individual Ca^{2+} channel types, we bath-applied type-specific blockers for HVA Ca^{2+} channels while evoking Ba^{2+} currents with depolarizing pulses (Fig. 1 *C* and *D Inset*). L-, N-, and P/Q-type currents were identified as currents sensitive to nifedipine, ω-conotoxin-GVIA, and ω-agatoxin-IVA (ω-Aga-IVA) (22). The remaining Cd^{2+}-sensitive current was taken as R-type current. Little or no Ba^{2+} current could be detected after application of 100 μM Cd^{2+}. There was no significant activity of T-type Ca^{2+} channels under our recording conditions. All four FHM1 mutations resulted in substantial reduction of the P/Q-type current density (Fig. 1*D*), consistent with our previous study (18). In contrast, L-, N-, and R-type current densities were not significantly different among the neurons expressing WT or FHM1 mutant channels (Fig. 1*D*). Thus, other HVA Ca^{2+} channels did not compensate for the deficit in P/Q-type channel activity in whole-cell recordings.

The reduction of overall somatodendritic Ca^{2+} influx in response to depolarization may have important functional implications. For example, in the *Rolling Nagoya* mouse, attenuation of P/Q-type current in Purkinje neurons causes deficits in generating Ca^{2+} spikes and subsequent bursts of Na^{+} spikes that would be seen in $\alpha_{1A}^{+/+}$ mice (25). In other neurons, inhibition of N- or P/Q-type

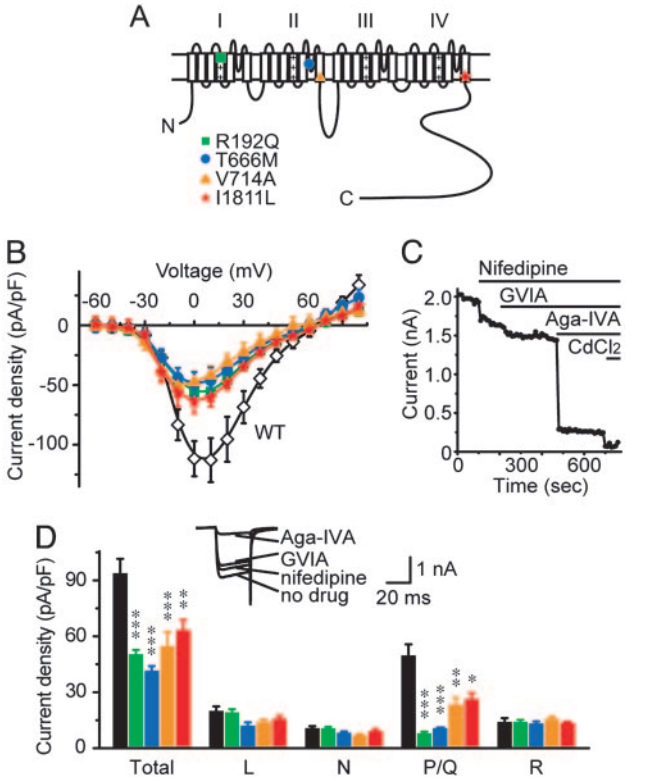

Fig. 1. Total and P/Q-type Ba^{2+} currents are both reduced in neurons expressing FHM1 mutant channels. (*A*) Topology of human α_{1A} subunit showing the four original FHM1 mutations. (*B*) Ba^{2+} I-V relationship in $\alpha_{1A}^{-/-}$ neurons expressing various human α_{1A} subunits. Total Ba^{2+} current densities were smaller in neurons expressing FHM1 mutant channels rather than WT α_{1A} ($P < 0.05$, 0 to +50 mV, $n = 10$–17). (*C*) Peak Ba^{2+} current vs. time for an exemplar WT-expressing neuron depolarized from −80 mV to +10 mV every 10 s. Pharmacological dissection of HVA Ca^{2+} channel currents by application of nifedipine (10 μM), ω-conotoxin-GVIA (2 μM), ω-Aga-IVA (1 μM), and $CdCl_2$ (100 μM). (*D*) Current density of total or individual HVA Ca^{2+} channel type, determined with the protocol in *C*, from $\alpha_{1A}^{-/-}$ neurons expressing various human α_{1A} subunits. (*Inset*) Averaged Ba^{2+} current traces of the neuron in *C*. In all mutant groups, total and P/Q-type current densities were smaller than WT ($n = 10$–19) but L-, N-, and R-type current densities were similar across all groups. *, $P < 0.05$; **, $P < 0.01$; ***, $P < 0.001$, all compared with WT group, in Figs. 1–5.

Ca^{2+} channels attenuates Ca^{2+}-dependent afterhyperpolarizations, thereby promoting spike generation (26).

Properties of WT and Mutant P/Q-Type Channels in Hippocampal Neurons. We went on to characterize some key biophysical properties of FHM1 mutant channels, again using ω-Aga-IVA sensitivity to identify P/Q-type current. First, we looked for shifts in voltage dependence of activation. Despite sharp reductions of current density in the mutant channels, the overall shape of the current–voltage relationship did not change appreciably (18). Possible displacements in the voltage dependence of activation were studied in greater detail by analysis of tail currents (Fig. 2*A*). Tails of P/Q-type current were evoked by repolarizing steps to −80 mV after brief depolarizing steps to various voltage levels. The FHM1 mutants displayed a hint of a small negative shift of the midpoint voltage of the activation curve ($V_{50,tail}$) but this failed to reach statistical significance by ANOVA (Table 1, which is published as supporting information on the PNAS web site). None of the mutant channels displayed a depolarizing shift; thus, displacements in voltage dependence were not responsible for the overall decrease of current density.

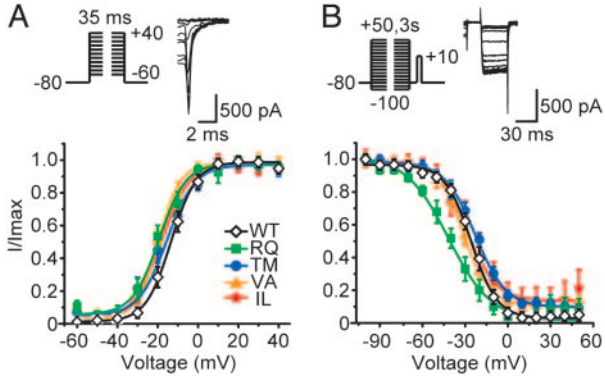

Fig. 2. Voltage-dependent gating of WT and mutant P/Q-type channels. (*A*) Activation was studied with tail currents (protocol, *Upper*). Exemplar current records were from a neuron expressing WT α_{1A}, with 3 MΩ uncompensated series resistance. Amplitudes of tail currents were normalized to the largest tails and data were fitted by a single Boltzmann function. No difference in $V_{50,tail}$ was found between WT and FHM1 mutant channels (n = 7–14, Table 1). (*B*) Inactivation was studied with voltage protocol shown (*Upper*). Exemplar records were from a neuron expressing WT α_{1A}. Amplitudes of currents elicited by test pulses were normalized to the largest current and fitted by a single Boltzmann function. The $V_{50,inact}$ and slope factor were significantly different between WT and RQ, but not between WT and any of the other FHM1 mutants (n = 5–10, Table 1).

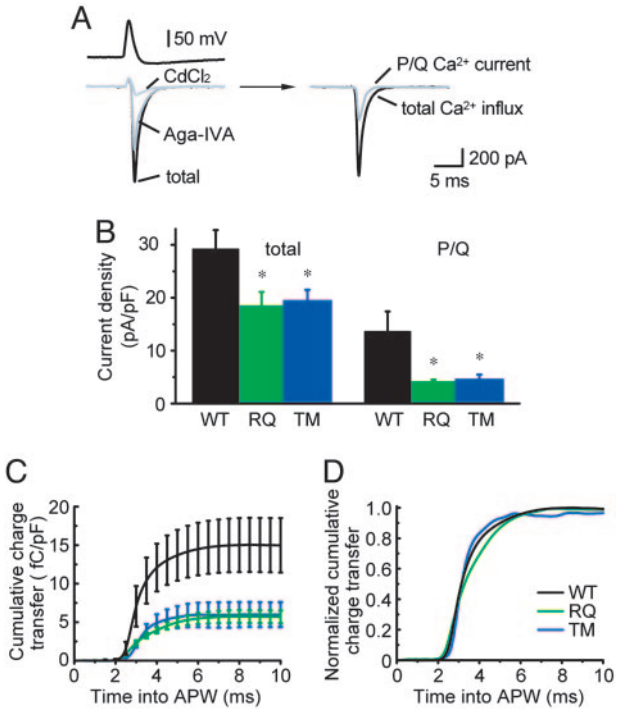

Fig. 3. Ca^{2+} influx evoked by APW command is reduced in neurons expressing FHM1 mutant channels. (*A*) Ca^{2+} current traces in $\alpha_{1A}^{-/-}$ neuron expressing WT α_{1A}. (*Left Upper*) APW derived from spontaneous action potentials. (*Left Lower*) Ca^{2+} current traces before and after drug applications. (*Right*) Total Ca^{2+} influx (difference between total current and current with $CdCl_2$) and P/Q Ca^{2+} current (difference between records before and after exposure to ω-Aga-IVA). (*B*) Total (*Left*) and P/Q-type (*Right*) peak current densities evoked by APW stimuli (n = 5–7). (*C*) Cumulative Ca^{2+} transfer through P/Q-type channels vs. time. (*D*) Normalized cumulative charge transfer showing no difference in timing of Ca^{2+} influx.

Second, we examined voltage-dependent inactivation in WT and mutant channels with a two-pulse protocol. Three-second prepulses to various potentials were followed by a fixed voltage pulse to +10 mV to elicit Ba^{2+} influx through the channels that remained available after the prepulse inactivation. The voltage dependence of inactivation followed a typical Boltzmann curve (Fig. 2*B*). Only the RQ mutant showed a negative shift in midpoint voltage ($V_{50,inact}$) of ~15 mV ($P < 0.01$) and a substantial decrease in steepness ($P < 0.05$, Table 1). Because the expression levels of WT and mutant α_{1A} are comparable (18), changes in the other aspects of P/Q-type channel biophysical properties may contribute to the deficit caused by FHM1 mutations. Our preliminary experiments on TM mutant indicate that the deficit in whole-cell current can be traced to a loss of gating charge movement in mutant channels, sharply diminishing the abundance of functionally gating channels per unit surface a_{1A} protein (C. F. Barrett, Y.-Q.C., and R.W.T., unpublished data).

Precedent for a deficit in channel activity without overt alterations in the voltage dependence of channel gating or in channel protein levels comes from the ataxic mouse *leaner* (tg^{la}). A mutation in the C terminus of mouse α_{1A} significantly reduces P/Q-type Ca^{2+} currents in tg^{la} cerebellar Purkinje cells (27, 28), without detectably lowering of α_{1A} mRNA or protein (29). In mice lacking α-neurexin, a functional weakening of N-type Ca^{2+} channels is observed despite the normal surface abundance of the channel protein (30).

FHM1 Mutations Reduce Ca^{2+} Influx Triggered by APWs. Next, we tested whether FHM1 mutations diminished Ca^{2+} influx under spiking conditions relevant to neurotransmission. Ca^{2+} channels were activated by an experimentally derived APW (Fig. 3*A*), not a rectangular pulse, and the permeant ion was Ca^{2+}, not Ba^{2+}. Ion fluxes through Na^+ and K^+ channels were blocked pharmacologically. The APW command elicited an inward Ca^{2+} current that peaked during the repolarization phase (31). The inward current surge was diminished by ω-Aga-IVA and nearly eliminated by Cd^{2+} (Fig. 3*A*). The peak P/Q-type Ca^{2+} influx was significantly smaller for RQ and TM than for WT, a reduction averaging >60% (Fig. 3*B Right*). This difference was clear in running integrals of charge transfer (Fig. 3*C*), which also showed that the timing of the normalized Ca^{2+} influx was not different between mutant and WT (Fig. 3*D*).

FHM1 Ca^{2+} Channels Are Deficient in Mediating Inhibitory Neurotransmission. The efficiency of neurotransmission depends critically on HVA Ca^{2+} channels positioned close to vesicular release sites. We have reported that FHM1 mutant channels are impaired in mediating excitatory transmission, in close accord with their deficiency in supporting Ca^{2+} channel activity (18). Here, we describe the effect of FHM1 mutations on inhibitory neurotransmission. We expressed various α_{1A} constructs in low-density $\alpha_{1A}^{-/-}$ hippocampal cultures and studied transmission from transfected neurons to nearby untransfected neurons with paired patch–clamp recordings at 12–18 DIV. Inhibitory connections constituted ~20% of the 350 synaptically connected pairs of neurons that we studied. In contrast to EPSCs, the IPSCs were larger, decayed much more slowly, and were completely blocked by 10 μM bicuculline (data not shown).

We defined the relative contributions of N-, P/Q-, and R-type Ca^{2+} channels to inhibitory transmission with sequential and cumulative application of specific channel blockers (Fig. 4*A*). Each toxin produced a crisp and maintained reduction in IPSC size. With all three toxins present, no remaining synaptic transmission could be detected, as confirmed by further application of bicuculline (data not shown). The contribution of L-type Ca^{2+} channels to IPSCs was negligible (data not shown) (32). Inhibitory transmission between $\alpha_{1A}^{-/-}$ neurons (ko group) was predominantly mediated by N-type channels (96 ± 1%, Fig. 4*B*).

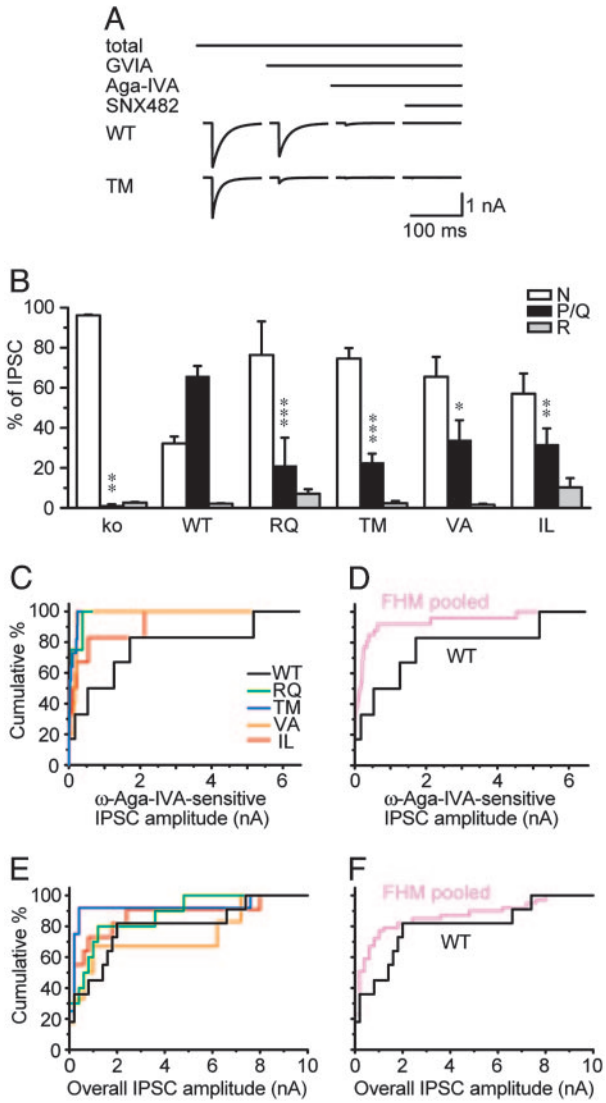

Fig. 4. FHM1 mutant channels are deficient in mediating inhibitory synaptic transmission. (*A*) Averaged IPSC traces from $\alpha_{1A}^{-/-}$ neurons expressing WT or TM α_{1A}. Sequence of drug application (2 μM ω-conotoxin-GVIA, 1 μM ω-Aga-IVA, and 0.5 μM SNX482) and effect of toxins was as indicated. (*B*) Corresponding contributions of N-, P/Q-, and R-type channels to IPSC amplitude (protocol as in *A*). Compared with WT, FHM1 mutant channels were each deficient in their ability to support IPSCs (n = 4–11). (*C*) Cumulative distributions of ω-Aga-IVA-sensitive IPSC amplitude from neurons in *B*. IPSCs supported by TM mutant (n = 11) were significantly smaller than those supported by WT (n = 6, $P < 0.05$). Other differences were not significant. (*D*) IPSCs pooled from all FHM1 groups (n = 26) were significantly different from WT ($P < 0.05$). (*E* and *F*) Overall IPSC amplitude distribution was similar at synapses expressing WT or mutant P/Q-type channels (*E*, n = 6–11); even when data from all FHM1 groups were pooled (n = 31) for comparison with WT (*F*, n = 8).

At synapses expressing WT human α_{1A} (WT group), N-type channels accounted for ~30% of the IPSC, whereas ω-Aga-IVA blocked 66 ± 5% of the synaptic transmission, not significantly different ($P > 0.15$) from that in $\alpha_{1A}^{+/+}$ neurons (54 ± 7%, see Fig. 6, EGFP group). In either case, blocking R-type channels had little additional effect. Thus, expression of WT human α_{1A} subunits at $\alpha_{1A}^{-/-}$ inhibitory synapses restored the normal contribution of P/Q-type channels to IPSCs (see also ref. 18). In contrast to endogenous mouse or WT human P/Q-type channels, FHM1 mutant channels were handicapped in mediating inhibitory transmission, supporting only 20–30% of the IPSC rather than ~60%. Instead, N-type channels dominated transmission in nerve terminals expressing mutant channels, just as in $\alpha_{1A}^{-/-}$ synapses. The mutations most sharply reducing Ca^{2+} channel activity, RQ and TM, also produced the largest reduction in P/Q-dependent GABAergic transmission (Fig. 4*B*).

Absolute IPSC amplitudes are compared in Fig. 4 *C* and *D*. Median amplitudes of P/Q-mediated IPSCs seemed smaller for each of the FHM1 mutants, but this difference only reached statistical significance for TM, the mutation with the largest sample size (n = 11). Only four to six inhibitory presynaptic neurons were obtained for the other mutants, reflecting the small number of inhibitory neurons in hippocampal cultures. To circumvent the paucity of inhibitory connections, we pooled data from all of the FHM1 mutants (n = 26, Fig. 4*D*) and found a significantly smaller P/Q-mediated component of the IPSC than at WT inhibitory synapses ($P < 0.05$). All in all, the data in Fig. 4 *B–D* indicated that FHM1 mutant channels were less capable than WT channels in supporting IPSCs.

$GABA_B$ Receptor-Mediated Inhibition Is Enhanced at Synapses Expressing FHM1 Mutant Channels. In contrast to P/Q-mediated IPSC component, the overall IPSC size did not differ between synapses expressing WT or FHM1 mutant Ca^{2+} channels (Fig. 4*E*), even when data were pooled from all four FHM1 mutants (Fig. 4*F*). We also examined paired-pulse depression (PPD) as a gauge of vesicle release probability (P_r), by applying pairs of stimuli 200 ms apart. PPD was not different between neurons expressing WT or FHM1 mutant channels (Table 2, which is published as supporting information on the PNAS web site), suggesting that P_r was well maintained at FHM1 mutant-expressing synapses, in line with the preservation of IPSC amplitude. All in all, expressing FHM1 mutant channels at inhibitory synapses resulted in changes of neurotransmission similar to what we observed at excitatory synapses (18): despite the consistent tilt away from P/Q-type channels and toward N-type channels, overall synaptic strength was maintained.

Could the changes at synapses expressing FHM1 mutant channels be pathogenic despite the apparent preservation of synaptic strength? One possibility is that frank alterations in synaptic strength do take place at certain synapses that regulate pain transmission, by analogy to the synapse-to-synapse variability in *tottering* (*tg*) mice (33, 34), in which α_{1A} contains a missense mutation that decreases P/Q-type Ca^{2+} current (35). Alternatively, the switchover in dominant channel type could alter the susceptibility of neurotransmission to presynaptic modulation. N-type Ca^{2+} channels are much more responsive than P/Q-type channels to G protein modulation (36, 37); additionally, once asserted, inhibition of N-type channels is more resistant to voltage-dependent relief (38, 39). Indeed, Zhou *et al.* (40) have shown that transmission from parallel fibers to Purkinje neurons is more susceptible to G protein-coupled receptor modulation in *tg* cerebellum than in WT, presumably because of a tilt toward N-type Ca^{2+} channels. Finally, FHM1 mutations may also alter the sensitivity of P/Q-type channels to G protein modulation (41).

To test this idea, we compared the effect of baclofen on neurotransmission from $\alpha_{1A}^{-/-}$ synapses expressing WT, RQ, or TM α_{1A} subunits. Baclofen binds to $GABA_B$ receptors, causing $G_\beta\gamma$ subunits to inhibit N- and P/Q-type Ca^{2+} channels. At $\alpha_{1A}^{-/-}$ synapses (Fig. 5, ko group), 10 μM baclofen caused a >80% reduction of both IPSC and EPSC amplitudes that was largely reversed upon removal of the drug (data not shown). The baclofen effect was completely prevented by $GABA_B$ receptor antagonist CGP55845 (2 μM, data not shown). The inhibition of synaptic current was likely caused by baclofen acting presynaptically as indicated by previous work (42).

At $\alpha_{1A}^{-/-}$ inhibitory synapses expressing RQ or TM mutant α_{1A}, the concentration-response curves for baclofen inhibition of IPSC were shifted strongly leftward compared with synapses

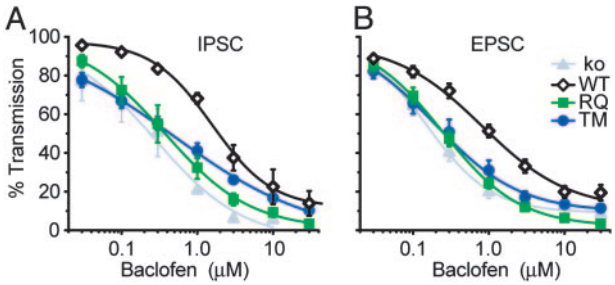

Fig. 5. Increased sensitivity to baclofen-induced inhibition at FHM1 mutant-expressing synapses. Concentration-response curves for baclofen-induced inhibition of IPSCs (*A*, $n = 3–4$) and EPSCs (*B*, $n = 6–8$) are shown. The curves were fitted by the Hill equation. IC_{50} values for RQ or TM were significantly lower than WT (Table 3).

expressing WT α_{1A} (Fig. 5*A*). IC_{50} values at RQ- and TM-expressing synapses were ~4-fold lower than WT and similar to that of $\alpha_{1A}^{-/-}$ synapses (Table 3, which is published as supporting information on the PNAS web site). Similar leftward shifts of baclofen concentration-response curves were also observed at excitatory synapses expressing RQ or TM mutant channels (Fig. 5*B* and Table 3). Thus, despite the apparent preservation of IPSC and EPSC amplitudes, both inhibitory and excitatory synapses grew much more responsive to neuromodulation when expressing FHM1 mutant rather than WT channels.

FHM1 Mutants Interfere with Endogenous Mouse P/Q-Type Channels in Mediating Inhibitory Synaptic Transmission. Our previous study showed that expression of FHM1 mutant channels in $\alpha_{1A}^{+/+}$ neurons reduced the overall contribution of P/Q-type channels to excitatory synaptic transmission, suggesting a competition between mutant and $\alpha_{1A}^{+/+}$ channels for type-preferring slots (18). Here, we tested whether similar interference took place for inhibitory synaptic transmission.

At $\alpha_{1A}^{+/+}$ synapses expressing EGFP alone, endogenous P/Q-type channels accounted for 54 ± 7% of inhibitory synaptic transmission (Fig. 6). When the presynaptic neurons additionally expressed FHM1 channels, this proportion was reduced to 19 ± 4% for RQ ($P < 0.001$) or 26 ± 6% for TM ($P < 0.05$). The impairment of P/Q-mediated synaptic currents at inhibitory synapses was very similar to that observed at excitatory ones (18). Thus, FHM1 mutant channels were able to hamper the participation of endogenous P/Q-type channels for both excitatory and inhibitory neurotransmission. However, the overall amplitude distribution of inhibitory synaptic current was no different in $\alpha_{1A}^{+/+}$ synapses expressing FHM1 mutants or EGFP alone ($P > 0.2$, data not shown).

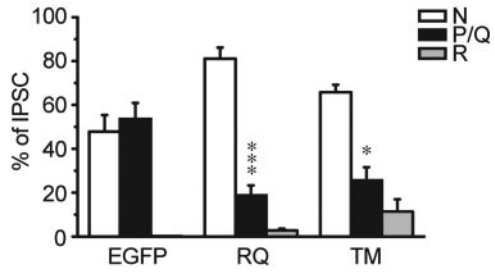

Fig. 6. "Dominant-negative effect" of FHM1 mutant channels in inhibitory $\alpha_{1A}^{+/+}$ hippocampal neurons. Contribution of P/Q-type channels to inhibitory neurotransmission was significantly diminished compared with EGFP group ($n = 4–7$; *, $P < 0.05$; ***, $P < 0.001$).

Discussion

FHM1 Mutations Reduce the Contribution of P/Q-Type Channels to Action Potential-Induced Ca^{2+} Influx and Inhibitory Transmission. We have described functional consequences of FHM1 mutations on inhibitory neurotransmission and their relationship to underlying changes in P/Q-type channel activity. The experiments were motivated by knowledge that inhibitory synaptic transmission plays a critical role in controlling the gain of circuits responsible for migraine headache (see below). We found that expression of FHM1 mutant channels in place of WT strongly and consistently reduced the contribution of P/Q-type channels to inhibitory transmitter release (Fig. 4). The effects on inhibitory synaptic transmission were in close accord with biophysical observations on alterations in P/Q-type channel activity for the four FHM1 mutations first described by Ophoff *et al.* (4).

Each of the original FHM1 mutants produced significantly less P/Q-type channel activity than WT human α_{1A} in whole-cell recordings, whereas the amplitudes of HVA Ca^{2+} currents supported by L-, N-, and R-type channels were no different (Fig. 1). The attenuation in P/Q current density at peak ranged from 50% to 80% relative to WT. In this respect our data are in good agreement with a previous study of FHM1 mutant channels expressed in cerebellar granule cells by Tottene *et al.* (17), who also found that FHM1 mutations decreased peak P/Q-type current. However, we did not detect a significant displacement of the midpoint voltage for voltage-dependent activation (Fig. 2 and Table 1), a notable difference because a negative-going shift in V_{50} has been proposed to allow FHM1 channels to carry larger Ca^{2+} fluxes than WT (13, 17, 20). When we tested this idea by monitoring Ca^{2+} currents in response to action potential-like command waveforms, simulating Ca^{2+} influx during neurotransmission, FHM1-expressing neurons were deficient in supporting Ca^{2+} entry (Fig. 3), just as found with Ba^{2+} currents and conventional step commands. Even if a small hyperpolarizing shift in V_{50} went undetected, the overall impact of FHM1 mutations on Ca^{2+} influx was attenuation, not potentiation. Thus, our data display a self-consistent pattern whereby FHM1 mutations produce concordant effects on conventional voltage–clamp analysis of Ba^{2+} currents, action potential-evoked Ca^{2+} influx and synaptic transmission in paired recordings (Figs. 1–4 and ref. 18). Further work will be needed to determine whether the discrepancies with refs. 17 and 20 arose from the use of different splice variants of α_{1A} or different expression systems.

Implications of Changes in P/Q-Type Ca^{2+} Channels for Migraine Pathophysiology. Scenarios for pain signaling must take into account both inhibitory and excitatory transmission. Stimuli that trigger migraine first activate primary afferent pain fibers that innervate the trigeminovascular system. This process in turn excites second-order projection neurons in the trigeminal nucleus caudalis (TNC), which then relay the signals to higher brain regions to generate headache (10). The efficiency of this ascending pain transmission pathway is tightly controlled at the level of TNC (43). Weakening of descending inhibition or local inhibitory feedback increases the gain of pain signaling (44). In a striking example (45), microinjection of ω-Aga-IVA into a key nucleus in the descending modulatory pathway, the periaqueductal gray, facilitates firing of TNC relay neurons, providing proof-of-principle that attenuation of P/Q-type channel activity can remove tonic descending inhibition and thereby enhance pain signaling.

Recent studies have highlighted the important influence of P/Q-type channels on inhibitory transmission *per se*. In tg^{la} mice, deficiency in P/Q-type channel activity weakens GABAergic inhibition of primary afferent pain fibers and heightens behavioral sensitivity to noxious heat (46). In rat trigeminal nucleus caudalis, local application of ω-Aga-IVA increased spontaneous

firing of nociceptive neurons, indicating that P/Q-type channels are important for tonic inhibitory modulation. No such effect of ω-Aga-IVA was seen with exogenous GABA present, indicating that the toxin acts by suppressing ongoing GABA release from inhibitory terminals (47). Our data complement these lines of evidence by showing that FHM1 mutations can diminish the contribution of P/Q-type channels to inhibitory neurotransmission, with the caveat that studies at exemplar synapses will need to be extended to synapses specifically implicated in migraine signaling.

One of our most striking findings was that the strength of basal inhibitory transmission can remain remarkably well preserved even with pronounced lessening of the role of P/Q-type channels. This overall constancy likely involves powerful compensatory mechanisms that make increasingly efficient use of the remaining Ca^{2+} influx, largely provided by N-type channels (18). Despite the preservation of basal transmission, a shift in reliance from P/Q- to N-type channels greatly increased susceptibility to presynaptic inhibition by G protein-mediated signaling (Fig. 5). Because migraine is an episodic disease, commonly triggered by emotional or physical stress, it would be reasonable to expect a heightened level of neuromodulation leading up to a migraine attack and, according to our findings, a state of weakened neurotransmission.

This work was supported by National Institutes of Health Grant NS24067 and the George D. Smith Professorship (to R.W.T.) and a Stanford Dean's Fellowship and Individual National Research Service Awards (to Y.-Q.C.).

1. Ferrari, M. D. (1998) *Lancet* **351,** 1043–1051.
2. Goadsby, P. J., Lipton, R. B. & Ferrari, M. D. (2002) *N. Engl. J. Med.* **346,** 257–270.
3. Ambrosini, A. & Schoenen, J. (2003) *Curr. Opin. Neurol.* **16,** 327–331.
4. Ophoff, R. A., Terwindt, G. M., Vergouwe, M. N., van Eijk, R., Oefner, P. J., Hoffman, S. M., Lamerdin, J. E., Mohrenweiser, H. W., Bulman, D. E., Ferrari, M., *et al*. (1996) *Cell* **87,** 543–552.
5. Mori, Y., Friedrich, T., Kim, M. S., Mikami, A., Nakai, J., Ruth, P., Bosse, E., Hofmann, F., Flockerzi, V., Furuichi, T., *et al*. (1991) *Nature* **350,** 398–402.
6. Starr, T. V., Prystay, W. & Snutch, T. P. (1991) *Proc. Natl. Acad. Sci. USA* **88,** 5621–5625.
7. Dunlap, K., Luebke, J. I. & Turner, T. J. (1995) *Trends Neurosci.* **18,** 89–98.
8. Catterall, W. A. (1998) *Cell Calcium* **24,** 307–323.
9. Tsien, R. W. & Wheeler, D. B. (1999) in *Calcium as a Cellular Regulator*, eds. Carafoli, E. & Klee, C. B. (Oxford Univ. Press, New York), pp. 171–199.
10. Welch, K. M. (2003) *Neurology* **61,** S2–S8.
11. Waeber, C. & Moskowitz, M. A. (2003) *Neurology* **61,** S9–S20.
12. Vanegas, H. & Schaible, H. (2000) *Pain* **85,** 9–18.
13. Pietrobon, D. & Striessnig, J. (2003) *Nat. Rev. Neurosci.* **4,** 386–398.
14. Kraus, R. L., Sinnegger, M. J., Glossmann, H., Hering, S. & Striessnig, J. (1998) *J. Biol. Chem.* **273,** 5586–5590.
15. Hans, M., Luvisetto, S., Williams, M. E., Spagnolo, M., Urrutia, A., Tottene, A., Brust, P. F., Johnson, E. C., Harpold, M. M., Stauderman, K. A. & Pietrobon, D. (1999) *J. Neurosci.* **19,** 1610–1619.
16. Kraus, R. L., Sinnegger, M. J., Koschak, A., Glossmann, H., Stenirri, S., Carrera, P. & Striessnig, J. (2000) *J. Biol. Chem.* **275,** 9239–9243.
17. Tottene, A., Fellin, T., Pagnutti, S., Luvisetto, S., Striessnig, J., Fletcher, C. & Pietrobon, D. (2002) *Proc. Natl. Acad. Sci. USA* **99,** 13284–13289.
18. Cao, Y. Q., Piedras-Renteria, E. S., Smith, G. B., Chen, G., Harata, N. C. & Tsien, R. W. (2004) *Neuron* **43,** 387–400.
19. Mullner, C., Broos, L. A., van den Maagdenberg, A. M. & Striessnig, J. (2004) *J. Biol. Chem.* **279,** 51844–51850.
20. van den Maagdenberg, A. M., Pietrobon, D., Pizzorusso, T., Kaja, S., Broos, L. A., Cesetti, T., Van De Ven, R. C., Tottene, A., Van Der Kaa, J., Plomp, J. J., *et al*. (2004) *Neuron* **41,** 701–710.
21. Zhuchenko, O., Bailey, J., Bonnen, P., Ashizawa, T., Stockton, D. W., Amos, C., Dobyns, W. B., Subramony, S. H., Zoghbi, H. Y. & Lee, C. C. (1997) *Nat. Genet.* **15,** 62–69.
22. Randall, A. & Tsien, R. W. (1995) *J. Neurosci.* **15,** 2995–3012.
23. Jun, K., Piedras-Renteria, E. S., Smith, S. M., Wheeler, D. B., Lee, S. B., Lee, T. G., Chin, H., Adams, M. E., Scheller, R. H., Tsien, R. W. & Shin, H. S. (1999) *Proc. Natl. Acad. Sci. USA* **96,** 15245–15250.
24. Fletcher, C. F., Tottene, A., Lennon, V. A., Wilson, S. M., Dubel, S. J., Paylor, R., Hosford, D. A., Tessarollo, L., McEnery, M. W., Pietrobon, D., *et al*. (2001) *FASEB J.* **15,** 1288–1290.
25. Mori, Y., Wakamori, M., Oda, S., Fletcher, C. F., Sekiguchi, N., Mori, E., Copeland, N. G., Jenkins, N. A., Matsushita, K., Matsuyama, Z. & Imoto, K. (2000) *J. Neurosci.* **20,** 5654–5662.
26. Bayliss, D. A., Li, Y. W. & Talley, E. M. (1997) *J. Neurophysiol.* **77,** 1362–1374.
27. Dove, L. S., Abbott, L. C. & Griffith, W. H. (1998) *J. Neurosci.* **18,** 7687–7699.
28. Lorenzon, N. M., Lutz, C. M., Frankel, W. N. & Beam, K. G. (1998) *J. Neurosci.* **18,** 4482–4489.
29. Lau, F. C., Abbott, L. C., Rhyu, I. J., Kim, D. S. & Chin, H. (1998) *Brain Res. Mol. Brain Res.* **59,** 93–99.
30. Missler, M., Zhang, W., Rohlmann, A., Kattenstroth, G., Hammer, R. E., Gottmann, K. & Sudhof, T. C. (2003) *Nature* **424,** 939–948.
31. Borst, J. G., Helmchen, F. & Sakmann, B. (1995) *J. Physiol. (London)* **489,** 825–840.
32. Takahashi, T. & Momiyama, A. (1993) *Nature* **366,** 156–158.
33. Caddick, S. J., Wang, C., Fletcher, C. F., Jenkins, N. A., Copeland, N. G. & Hosford, D. A. (1999) *J. Neurophysiol.* **81,** 2066–2074.
34. Matsushita, K., Wakamori, M., Rhyu, I. J., Arii, T., Oda, S., Mori, Y. & Imoto, K. (2002) *J. Neurosci.* **22,** 4388–4398.
35. Wakamori, M., Yamazaki, K., Matsunodaira, H., Teramoto, T., Tanaka, I., Niidome, T., Sawada, K., Nishizawa, Y., Sekiguchi, N., Mori, E., *et al*. (1998) *J. Biol. Chem.* **273,** 34857–34867.
36. Currie, K. P. & Fox, A. P. (1997) *J. Neurosci.* **17,** 4570–4579.
37. Zamponi, G. W. & Snutch, T. P. (1998) *Curr. Opin. Neurobiol.* **8,** 351–356.
38. Brody, D. L. & Yue, D. T. (2000) *J. Neurosci.* **20,** 889–898.
39. Currie, K. P. & Fox, A. P. (2002) *J. Physiol. (London)* **539,** 419–431.
40. Zhou, Y. D., Turner, T. J. & Dunlap, K. (2003) *J. Physiol. (London)* **547,** 497–507.
41. Melliti, K., Grabner, M. & Seabrook, G. R. (2003) *J. Physiol. (London)* **546,** 337–347.
42. Luscher, C., Jan, L. Y., Stoffel, M., Malenka, R. C. & Nicoll, R. A. (1997) *Neuron* **19,** 687–695.
43. Woolf, C. J. & Salter, M. W. (2000) *Science* **288,** 1765–1769.
44. Fields, H. L. & Basbaum, A. I. (1999) in *Textbook of Pain*, eds. Wall, P. D. & Melzack, R. (Elsevier, London), pp. 309–329.
45. Knight, Y. E., Bartsch, T., Kaube, H. & Goadsby, P. J. (2002) *J. Neurosci.* **22,** RC213:1–6.
46. Ogasawara, M., Kurihara, T., Hu, Q. & Tanabe, T. (2001) *FEBS Lett.* **508,** 181–186.
47. Ebersberger, A., Portz, S., Meissner, W., Schaible, H. G. & Richter, F. (2004) *Cephalalgia* **24,** 250–261.